

Optimized Process for the Inclusion of Carbon Nanotubes in Elastomers with Improved Thermal and Mechanical Properties

Rahul M. Cadambi, Elaheh Ghassemieh

Department of Mechanical Engineering, The University of Sheffield, Mappin Street, S13JD Sheffield, United Kingdom

Received 17 June 2011; accepted 7 September 2011

DOI 10.1002/app.35608

Published online 11 December 2011 in Wiley Online Library (wileyonlinelibrary.com).

ABSTRACT: The effects of addition of reinforcing carbon nanotubes (CNTs) into hydrogenated nitrile-butadiene rubber (HNBR) matrix on the mechanical, dynamic viscoelastic, and permeability properties were studied in this investigation. Different techniques of incorporating nanotubes in HNBR were investigated in this research. The techniques considered were more suitable for industrial preparation of rubber composites. The nanotubes were modified with different surfactants and dispersion agents to improve the compatibility and adhesion of nanotubes on the HNBR matrix. The effects of the surface modification of the nanotubes on various properties were examined in detail. The amount of CNTs was varied from 2.5 to 10 phr in different formulations prepared to identify the optimum CNT levels. A detailed analysis was made to investigate the morphological structure and mechanical

behavior at room temperature. The viscoelastic behavior of the nanotube filler elastomer was studied by dynamic mechanical thermal analysis (DMTA). Morphological analysis indicated a very good dispersion of the CNTs for a low nanotube loading of 3.5 phr. A significant improvement in the mechanical properties was observed with the addition of nanotubes. DMTA studies revealed an increase in the storage modulus and a reduction in the glass-transition temperature after the incorporation of the nanotubes. Further, the HNBR/CNT nanocomposites were subjected to permeability studies. The studies showed a significant reduction in the permeability of nitrogen gas. © 2011 Wiley Periodicals, Inc. *J Appl Polym Sci* 124: 4993–5001, 2012

Key words: carbon nanotube; elastomers; gas permeation; nanocomposites; TEM

INTRODUCTION

Elastomers are of great industrial importance because of their high and reversible deformability. Because of their low inherent tensile and tear strength, it is a common practice to reinforce elastomers with fillers to improve their mechanical properties. The most commonly used conventional filler materials are in the form of particles such as calcium carbonate, carbon black, and silica. The main drawback of these conventional fillers is that they need to be added in high amounts (ca. 30–70 wt %). These high filler levels may have some detrimental effects, such as increases in weight, brittleness, hardness, and opacity, in the resulting composites.^{1,2} With recent advancements in polymer/nanofiller composites, these limitations could be overcome by changes in the volume fraction, shape, and size of the fillers particles.³

Since the discovery of carbon nanotubes (CNTs) by Iijima,⁴ they have attracted a great deal of interest for improving various properties of base materials. CNTs are known to possess excellent electrical properties,⁵ a high aspect ratio, a high strength,⁶ and thermal conductivity.⁷ Despite substantial research by various researchers in recent years, the preparation of CNT-filled polymer composites faces significant technical difficulties with regard to the effective incorporation of CNTs into the polymer matrix. The two main important issues are the adequate dispersion of CNTs in the polymers and the creation of a strong interfacial bonding between the CNTs and the polymers. CNTs tend to aggregate together as a result of the strong van der Waals forces due to the large aspect ratio (>1000) of the tubes.

In this present study, we considered incorporating CNTs into hydrogenated nitrile-butadiene rubber (HNBR). Our work focused on the preparation of rubber-filled CNTs with formulations that were directly applicable to industrial environments. The main use of the produced nanocomposite elastomers from this research would be for seal applications to be used at high temperatures and pressures. In this work, HNBR/CNT nanocomposites were synthesized through various preparation methods. A novel

Correspondence to: E. Ghassemieh (e.ghassemieh@sheffield.ac.uk).

Contract grant sponsor: James Walker, Ltd., Cockermouth, United Kingdom.

TABLE I
DMTA Property Values of HNBR Nanocomposites

	M_c	v_c	Density (mg/m^3)	E' (GPa) at 25°C	T_g (°C)	Tan δ values at 25°C
H	6355	1.13×10^{20}	1.197	0.014	-16.7	0.184
HCNT3.5	4930	1.46×10^{20}	1.194	0.018	-14.5	0.210
HMB3.5	4663	1.54×10^{20}	1.192	0.019	-15.25	0.190
HMBDA3.5	3408	2.11×10^{20}	1.192	0.026	-14.25	0.230
HMBNaDBBS3.5	4212	1.7×10^{20}	1.190	0.021	-14.65	0.214

H, HNBR control sample; HCNT2.5, HNBR with 2.5phr CNTs nanocomposite sample; HCNT3.5, HNBR with 3.5phr CNTs nanocomposite sample; HCNT5, HNBR with 5phr CNTs nanocomposite sample; HCNT7.5, HNBR with 7.5phr CNTs nanocomposite sample; HCNT10, HNBR with 10phr CNTs nanocomposite sample; HMB3.5, HNBR with 3.5phr predispersed CNTs masterbatch nanocomposite sample; HMBDA3.5, HNBR with 3.5phr predispersed CNTs with dispersion agent masterbatch; nanocomposite sample; HMBNaDBBS3.5, HNBR with 3.5phr predispersed CNTs with surfactant masterbatch; nanocomposite sample.

approach of ultrasonic predispersion of the HNBR/CNT masterbatch was developed. The effects of surface modification with various dispersion agents (DAs) and surfactants are described. The structure of the nanocomposites was visualized by transmission electron microscopy (TEM). Mechanical tests of the prepared nanocomposites were carried out at room temperature to assess the potential effects of the addition of nanotubes in the HNBR matrix. The viscoelastic properties of the nanocomposites were investigated by dynamic mechanical thermal analysis (DMTA) tests. The CNT nanocomposites were subjected to permeability studies to evaluate the effect of the incorporation of the CNTs on the gas barrier properties.

EXPERIMENTAL

Materials

A fully saturated HNBR with a 36% nitrile content was used to prepare the CNT nanocomposites. James Walker Co, Ltd. (Cockermouth, United Kingdom), kindly supplied HNBR and other compounds in the recipes. The compounding procedure was followed as per James Walker's recipe. Multiwalled CNTs bearing the trade name NC7000 were procured from Nanocyl S. A. (Samberville, Belgium). Dow Corning (United Kingdom) kindly supplied us with the DA Z-6173 that was used for our trials. The technical-grade surfactant sodium dodecyl benzene sulfonate (NaDBBS) was purchased from Fisher Scientific (United Kingdom). Methyl ethyl ketone (MEK) used for swelling the rubber was also procured from Fischer Scientific.

Preparation of the HNBR/clay nanocomposites

The HNBR/CNT nanocomposites were prepared through a technique that is more suitable to conventional industrial production. The mixing techniques and rubber preparation protocols were done strictly

according to James Walker's preparation procedures. Accordingly, all of the CNT nanocomposites were prepared by a conventional shear mixing method. The addition of CNTs was carried out by two means. One involved the dry addition of CNTs, and the other used a novel technique of ultrasonic predispersion of the rubber/CNT masterbatch. The amount of CNTs was varied from 2.5, 3.5, 5, and 7.5 to 10 phr to optimize the CNT filler levels in the rubber matrix. The rubber/CNT masterbatch preparation was carried out as follows. Initially, HNBR was swollen in MEK. Later, the CNTs were added to a separate MEK solvent and stirred continuously to obtain a uniform mixture. Both the CNT mixture and the swollen HNBR mixture were subjected to ultrasonication for certain period with a Branson sonifier 450 (Danbury, CT, USA) composed of a solid titanium stepped horn. The HNBR/CNT masterbatch mixture was spread out on a flat sheet after sonication and was kept *in vacuo* at room temperature. The dried rubber/CNT masterbatch was used for the preparation of the nanocomposite samples. Separate HNBR/CNT masterbatches were prepared in a similar way as described previously by the addition of optimized percentages of DA and surfactant (NaDBBS) to investigate the effect of various coupling agents.

The nanocomposites were prepared with a laboratory-scale Francis Shaw K0 intermix (Lancashire, UK) operated at a speed of 25 rpm for a period of 5 min. The CNTs, both dry CNTs and predispersed rubber/CNT masterbatches, were added to the mixing chamber along with other compounding materials to obtain the nanocomposites. The amount of CNT loadings was varied by 2.5, 3.5, 5, 7.5, and 10 phr to optimize the addition levels of CNTs. The material dropped out from the mixer was passed through a two-roll mill. All of the rubber test sheet samples were cured as per ISO 471, that is, for 6 min at 185°C. The abbreviations used for different formulations prepared and characterized in this research are given in detail in Table I, along with the DMTA properties.

Characterization

Morphological studies

High-resolution TEM analysis was performed on an FEI Technai G2 FEG TEM instrument (Eindhoven, Netherlands) operated at an accelerating voltage of 100 kV. The nanocomposite samples were initially frozen to -100°C before cryomicrotomy was performed. The initial coarse sectioning was carried out with freshly cut glass knives with a cutting edge of 45° . Fine and shiny cryosections approximately 60 nm thick were sliced with a Diatome Cryotrim 35° diamond knife. The ultrathin sections were carefully placed on a 200 Formvar mesh, otherwise known as polyvinyl formal support film grids, for observation under TEM.

Mechanical testing

Tensile testing was performed as per BS 903 part A2/ISO 37. The dumbbell-shaped tensile specimens were cut according to BS 903 type 2 specification. Tensile testing was carried out at room temperature on a Tinius Olsen H10K-T UTM instrument with a load of 500 N at a crosshead speed of 500 mm/min. An average of at least five measurements was tested and reported for each composition of the HNBR/CNT nanocomposites.

DMTA

Dynamic mechanical studies of the nanocomposite samples were carried out on Metravib VA2000 DMTA instrument (Linonest, France) in tensile mode at a constant frequency of 1 Hz and a strain rate of 0.01% for a wide range of temperatures from -80 to 80°C at a heating rate of $2^{\circ}\text{C}/\text{min}$. The storage modulus (E') and loss factor ($\tan \delta$) were measured as a function of temperature for all of the samples under identical conditions. The glass-transition temperature (T_g) of the samples was calculated from the respective $\tan \delta$ peak.

Permeability tests

The main objective of our work was to develop a novel O-ring seal material that could withstand high temperatures and high pressures in harsh environmental conditions. Reducing the permeability of a gas is one of the essential requirements for rubber seals. The permeability tests were carried out as ISO 2872 : 2006. This test method determined the rate of gas transmission through elastomer with respect to temperature and pressure. The test sample was cut in the shape of an O-ring with a cross-sectional area of 24 cm^2 with a thickness of 2 mm. The test sample was mounted between a hollow cylinder. The chamber was then filled with nitrogen gas until a test pressure of 8 bar and a temperature of 80°C were achieved.

The drop in pressure over time was recorded after 15, 30, and 60 min and then for every hour up to 3 h. The pressure gradients recorded were plotted according to the variation of pressure with respect to time. The pressure gradients were extrapolated for longer time durations with trend-fitting techniques. With the ideal gas law equation, the volume loss per second depending on the pressure was calculated. Permeability curves were plotted with the volume loss per second values obtained depending on the pressure. Finally, the permeability coefficient (Q) values were calculated with the slope of the permeability curves.

RESULTS AND DISCUSSION

Surface modification of the CNTs

It is well known that the dispersion of CNTs in a rubber matrix is a big challenge. We decided to carry out the surface modification of CNTs to improve the adhesion of the CNTs and thereby help to provide uniform dispersion in the rubber matrix. The first and basic requirement of surface modification of CNTs is to perform a solubilization test in the solvent. The as-received dry CNT powder was incorporated into the solution of MEK and sonicated to obtain a uniform mixture. Separately, CNTs with DA and surfactant (NaDBBS) were added to MEK and sonicated. After centrifugation, the solution looked like a black solution. All of the mixtures were kept for a week to check whether there was any sediment deposition of CNTs and coupling agents in the mixture. After 1 week, the intense coloration of the CNT mixture was retained, and we observed no sedimentation of CNTs at the bottom of the glass beaker. Furthermore, the CNTs were observed under SEM to check whether there was any damage on the CNT walls due to sonication before preparation of the nanocomposites.

Figure 1(a) shows the CNTs in as-received condition at different magnification levels. Highly coiled and entangled CNT particles as received are shown in Figure 1(a) at different levels of magnification. Figure 1(b) shows the SEM images of the CNTs after sonication. As mentioned before, sonication was performed on the CNTs to obtain a uniform mixture of solvent along with the surface modifiers. In Figure 1(b), we clearly observed a reduction in the entanglements of the CNTs. This modification might have aided in providing a better separation of CNTs during incorporation into the rubber matrix. Further, this might have helped provide better dispersion and adhesion to the polymer matrix.

Microstructural characterization

Microstructural analysis was performed to obtain insight into the level of dispersion of the CNTs in

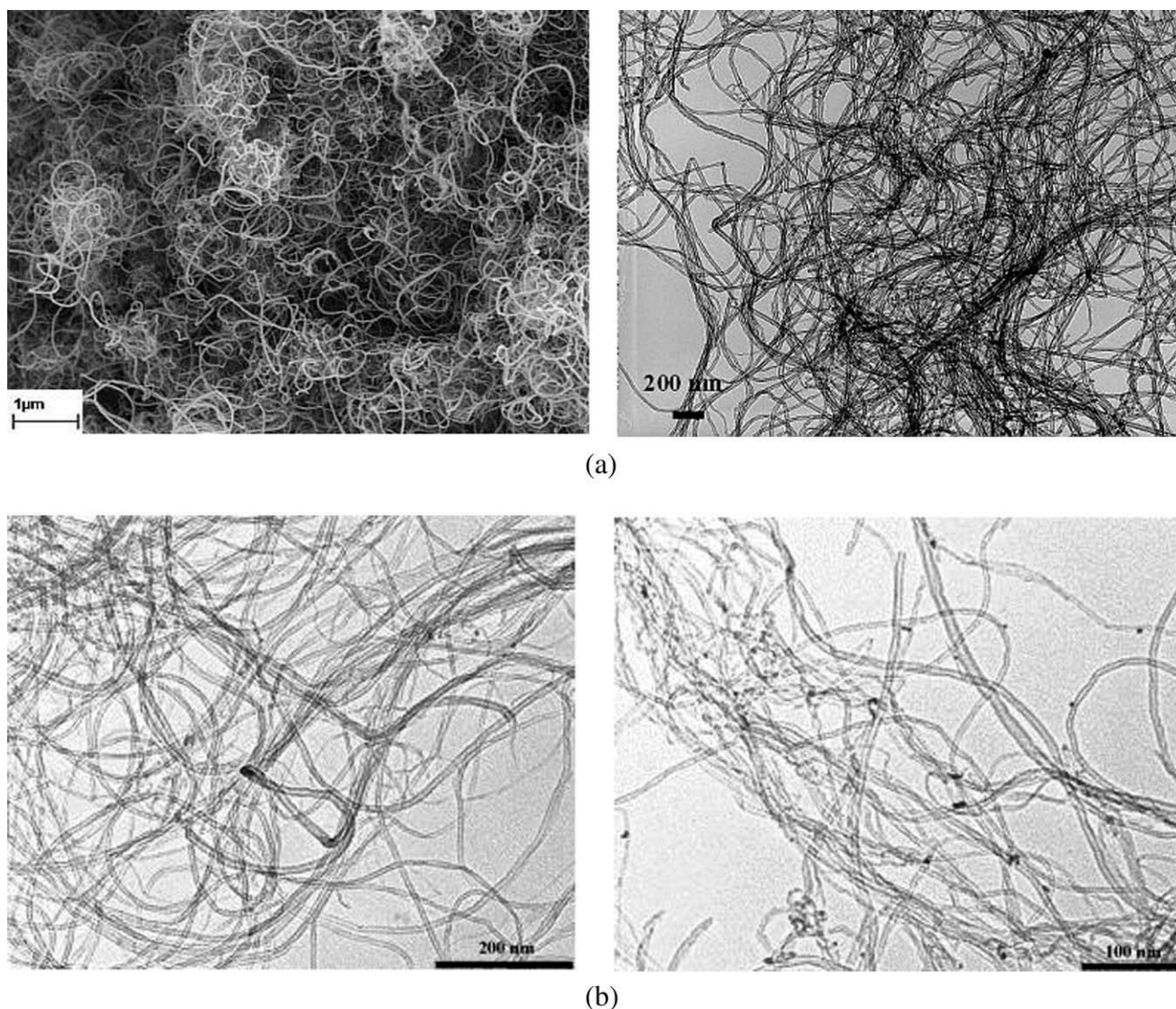


Figure 1 TEM image of the CNTs in (a) as-received condition and (b) after sonication.

rubber matrix. The prepared nanocomposite samples were characterized by TEM. TEM microphotographs of various prepared HNBR/CNT nanocomposites are shown in Figure 2(a–f). Figure 2(a–d) shows samples of the CNT nanocomposite having 2.5-, 3.5-, 5-, and 10-phr levels of CNTs, respectively. It can be observed in Figure 2 that there was an increasing agglomeration of CNTs with the increase in loading levels. With a 10-phr level of CNTs [Fig. 2(d)], there was a clear indication of CNT agglomeration, which is marked in the TEM image [Fig. 2(d)]. For the nanocomposites with 2.5- and 3.5-phr levels of CNTs, as shown in Figure 2(a,b), there was good separation of CNT bundles with no sign of agglomeration. At 5-phr levels, even though there was good separation of the CNT bundles, there were areas with CNT entanglements that failed to uncoil [as depicted in Fig. 2(c)]. TEM

analysis showed that 2.5 and 3.5 phr were the optimum loading levels of the CNTs for our formulation.

Cassagnau et al.⁸ reported that the surface modification of the CNT surface results in better dispersion of CNTs in the corresponding polymer matrix. Also, Verge et al.⁹ reported that there is enhanced dispersion and adhesion of CNTs with a relatively higher acrylonitrile (ACN) content in the elastomer matrix. This might be one of the strong reasons for our observations of very good and uniform dispersion of CNTs with the HMBDA3.5 [Fig. 2(e)] and HMBNaDBBS3.5 [Fig. 2(f)] set of samples. The TEM images generally showed that the optimum CNT level was 3.5 phr. With the use of the predispersion technique and with suitable surface modification, there was a more uniform dispersion of CNTs in the HNBR matrix.

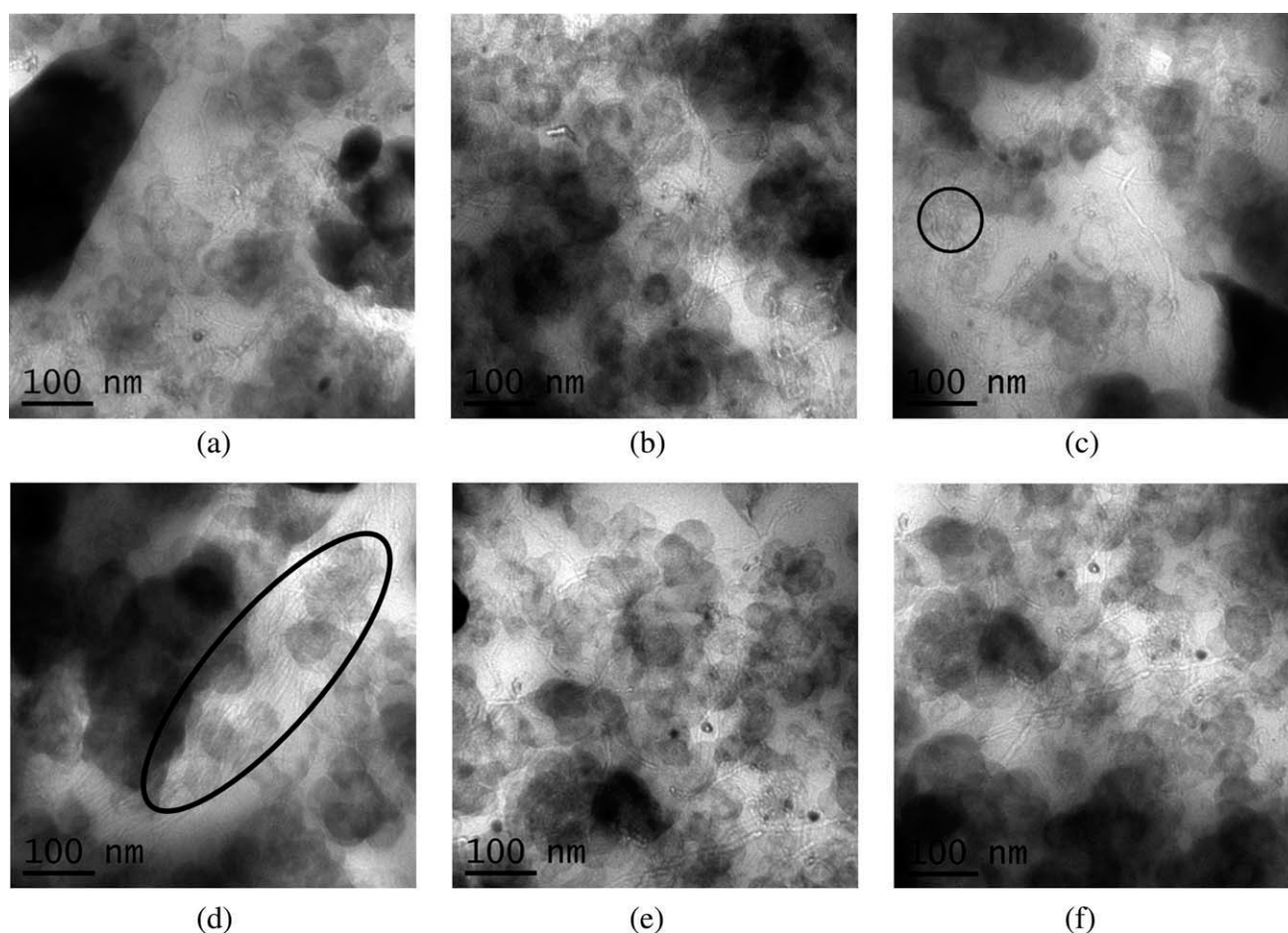


Figure 2 TEM images of (a) HCNT2.5 (b) HCNT3.5 (c) HCNT5 (d) HCNT10 (e) HMBDA3.5 and (f) HMBNaDBBS3.5.

DMTA

The dynamic mechanical properties of the control sample and various nanocomposites at 3.5-phr levels were studied over the temperature range of -80 to 80°C . The plots of the $\tan \delta$ and E' are shown in Figure 3(a,b), respectively. The T_g , E' , and $\tan \delta$ values at 25°C and other DMTA properties are tabulated in Table I.

The $\tan \delta$ peak corresponded to T_g of the nanocomposite sample. From Figure 3(a), we observed that after the CNTs were reinforced, there was a reduction in the $\tan \delta$ peak with a shift in T_g to lower temperature values. Various other researchers have observed and reported this sort of behavior.^{10,11} We observed a shift in T_g by 2.2°C with the direct mixing of CNTs and up to 2.25°C after we used various coupling agents. The shift in the T_g values took place only when there was a reduction in the mobility of the polymer chain molecules. This clearly indicates that strong adhesion created between CNTs and rubber chain molecules resulted in a decrease in the T_g values. Wang¹² and López-Manchado et al.¹⁰ explained that the reduced mobility of polymer chains after the incorporation of

CNTs is due to the fact that interaction of CNTs restricts the mobility of the elastomer segments, and this significantly shifts T_g to higher temperatures. The rubber portion immobilized acts as a part of the filler rather than the polymer and increases the effective volume of the filler.^{10,12}

It is interesting to note from Figure 3(a) that the samples HMBDA3.5 and HMBNaDBBS3.5 showed the lowest $\tan \delta$ peaks with more shifting in T_g (Table I) when compared to the other set of samples. This suggests that with the use of coupling agents, there was much stronger reinforcement of CNTs with rubber chains. This improvement could be attributed to the predispersion technique and modification of the CNT surface. Also, the $\tan \delta$ values reported in Table I show the increase with the addition of the CNTs. Therefore, we expect that the addition of the CNTs improved the energy absorption capability of the elastomer.

Figure 3(b) shows the E' values for various HNBR/CNT samples in comparison with the control sample for a temperature range from -80°C to $+80^{\circ}\text{C}$. The E' values for various samples are tabulated in Table I. It should be noted that E' reflects the elastic modulus of a rubber material and measures the recoverable strain energy in a deformed specimen.¹³ It can be observed

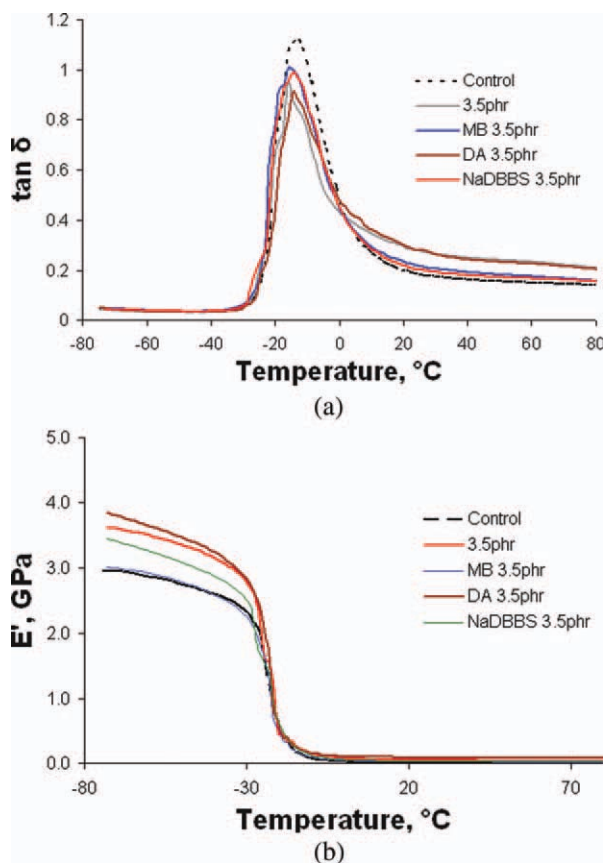


Figure 3 DMTA results of the HNBR/CNT nanocomposites: (a) $\tan \delta$ and (b) E' (MB, masterbatch). [Color figure can be viewed in the online issue, which is available at wileyonlinelibrary.com.]

from Figure 3(b) and Table I that there was a good increase in E' after the addition of CNTs into HNBR. This increase in E' could be attributed to hydrodynamic reinforcement upon introduction of the filler.¹⁴ It is well known that CNTs possess a high surface-to-volume ratio and high mechanical stiffness. Because of the large interfacial area and stronger polymer–filler interaction,¹⁵ there was a possibility of reduced mobility in the rubber chains. This immobilized rubber acted as a filler and, hence, increased the effective volume of filler loading and gave rise to higher hysteresis at higher temperatures and lower hysteresis at lower temperatures.¹⁰

To get a clear indication on the DMTA results, the apparent crosslink density (ν_c) was calculated with the formulas given and are tabulated in Table I. When a material is sufficiently crosslinked to form a solid with a reasonable degree of mechanical integrity above the glass rubber transition, DMTA can be used to estimate its crosslink density with the following formula:

$$E = \frac{3\rho RT}{M_c}$$

where E is the equilibrium shear modulus at 298 K, ρ is the density, R is the universal gas constant (8.314 J/K. mol), T is the thermodynamic temperature (298 K), and M_c is the molecular mass between crosslinks. ν_c can be measured by

$$\nu_c = \frac{N\rho}{M_c}$$

where N is Avogadro's number (6.023×10^{23}). It should be noted that M_c and ν_c are apparent values.¹⁶ These values give a clear indication of the rubber–filler and filler–filler interactions.¹⁶ From Table I, we can clearly observe that there was a good increase in the crosslink density values at 3.5-phr levels.

Mechanical properties

It is known that elastomers are reinforced with fillers; this leads to improvement in various desired mechanical properties. So, tensile tests are most widely used to evaluate the extent of dispersion of fillers in the rubber matrix. Figure 4(a) shows the

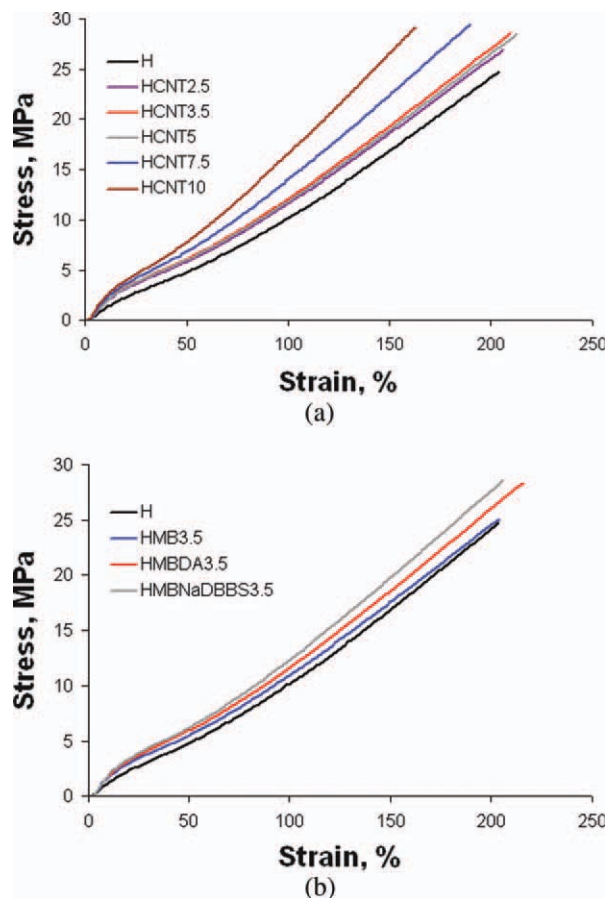


Figure 4 Stress–strain curves of various HNBR/CNT nanocomposites: (a) without coupling agents and (b) with coupling agents. [Color figure can be viewed in the online issue, which is available at wileyonlinelibrary.com.]

TABLE II
Mechanical Properties of the Various HNBR/CNT Nanocomposites

Sample	Tensile strength (MPa)	Elongation at break (%)	Modulus at 50% (MPa)	Modulus at 100% (MPa)
H	26.6 ± 0.74	204 ± 11	3.37 ± 0.15	9.07 ± 0.38
HCNT2.5	26.9 ± 0.66	206 ± 10	5.81 ± 0.12	13.65 ± 0.41
HCNT3.5	28.6 ± 0.71	209 ± 9	6.89 ± 0.11	15.01 ± 0.36
HCNT5	28.5 ± 0.84	210 ± 11	6.83 ± 0.13	15.16 ± 0.47
HCNT7.5	29.5 ± 0.94	190 ± 12	5.43 ± 0.16	15.85 ± 0.51
HCNT10	29.2 ± 0.98	163 ± 12	8.34 ± 0.17	21.13 ± 0.62
HMB3.5	26.1 ± 0.68	205 ± 10	4.86 ± 0.14	12.35 ± 0.43
HMBDA3.5	27.3 ± 0.72	221 ± 11	5.16 ± 0.13	14.09 ± 0.50
HMBNaDBBS3.5	27.9 ± 0.73	220 ± 10	5.20 ± 0.11	14.48 ± 0.48

tensile stress–strain curves for various CNT-filled HNBR nanocomposites prepared by the direct addition method in comparison with standard HNBR. Various tensile properties, such as the tensile strength, elongation at break, and moduli at 50 and 100% elongations, are tabulated in Table II. After the addition of 2.5 phr CNTs into HNBR, the tensile strength increased by 1.1%. With 3.5- and 5-phr levels of CNTs, the tensile strength improved by 7.5 and 6.9%, respectively. Also, the modulus at 100% elongation increased by 50.5, 65.5, and 67.1%, respectively, for 2.5, 3.5, and 5 phr levels of CNTs. Another interesting point to be noted is that the elongation at break was not much affected by the incorporation of CNTs. Such a significant increase in the stiffness is not commonly observed in conventional fillers such as carbon black or other reinforcing fillers. This significant increase in the level of the mechanical properties was mainly due to the high length-to-diameter ratios of the CNTs. It is well known that improvements in the tensile properties can be attributed to the degree of crosslinking in the polymer and the level of polymer–filler interactions. It could be assumed that with a lower level of loading, that is, 2.5 and 3.5 phr CNTs, the physical interaction between the HNBR chain molecules and CNTs were stable. Because of the large-scale aspect ratio of CNTs, they can encourage additional physical crosslinks in the elastomer network and, thereby, result in improved tensile properties. Also, it has been reported that ACN groups¹⁵ have a strong inherent affinity to nanotubes. Also, Verge et al.⁹ reported that it can be imagined that during the conventional shear mixing technique of CNTs and HNBR, the ACN units spread along the elastomer chains and tend to organize and localize preferentially around the nanotubes.

It is interesting to note that there was not much improvement in the tensile strength and modulus at 5-phr levels of loadings in comparison to 3.5-phr amounts of CNTs. The mechanical properties remained almost the same at both amounts of CNTs.

This suggests that 3.5 phr seemed to be the optimum level of loadings in the HNBR matrix under the process conditions used.

With the increase of CNT level to 7.5 and 10 phr, the tensile strength increased by 11 and 10%, respectively, and the modulus increased by 75 and 133%, respectively. However, in contrast, there were reductions in the elongation at break by 13.2 and 24.2%, respectively. This behavior could have mainly been due to the presence of aggregated bundles of CNTs in the polymer matrix (which was confirmed from TEM observations). After a certain level of elongation, the CNTs slipped from the polymer chains and resulted in premature breaking, and thus, there was a huge decrease in elongation at break compared to the control sample.

Figure 4(b) shows the tensile stress–strain curves of various HNBR/CNT nanocomposites prepared with the masterbatch technique in comparison to the standard sample. The tensile properties, along with the standard deviations, are also tabulated in Table II. Only the results of the samples with a 3.5-phr level of CNTs treated with various coupling agents are shown here. It was proven from our previous investigation that these samples contained the optimum level of CNT loading. The use of the surfactant (NaDBBS) and DA resulted in increases in the tensile strength by 2.6 and 4.9%, respectively. The elongation at break and modulus increased by 7.7 and 60%, respectively, with the help of the surfactant and DA. It is interesting to note that the increase in the elongation at break was around 7.7%, although the samples without any coupling agent for the same level of CNT loadings (3.5 phr) showed only an increase of 2.5% for the elongation at break. This clearly suggests that surface modification on CNTs led to the formation of additional chemical crosslinks other than the regular physical crosslinks at low levels of CNTs. Also, the improved mechanical properties were attributed to the predispersion technique employed for the addition of the CNTs in the HNBR matrix.

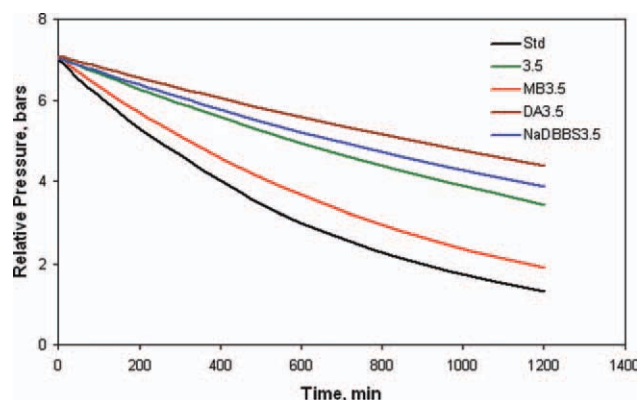


Figure 5 Trend-fitted relative pressure with respect to time for various 3.5-phr HNBR/CNT nanocomposites (Std, Control sample MB, masterbatch). [Color figure can be viewed in the online issue, which is available at wileyonlinelibrary.com.]

Permeability tests

Figure 5 shows the relative pressure plotted over time for various HNBR nanocomposite sample variants with a 3.5-phr level of CNTs. To evaluate the behavior of the elastomer samples, the experimental values were extrapolated with exponential trend-fitting curves.

Nitrogen gas was considered as the ideal gas, and permeability was determined with the ideal gas law equation. With the ideal gas law equation given next, dp/dt was calculated by the replacement of t in the derivative equation:

$$pV = nRT$$

$$V \frac{dp}{dt} = RT \frac{dn}{dt}$$

$$V \frac{dp}{dt} = \frac{RT dV}{V_m dt}$$

$$\frac{dV}{dt} = \frac{V_m V \frac{dp}{dt}}{RT}$$

where P is the pressure in Pa, t is time, secs, R is universal gas constant, V_m is Standard molar volume at STP and V is the volume of the test chamber. $V = 0.005 \text{ m}^3$, $R = 8.314 \text{ m}^3 \text{ Pa K}^{-1} \text{ mol}^{-1}$, $T = 333 \text{ K}$, and $V_m = 0.0224 \text{ m}^3/\text{mol}$.

The volume losses per second obtained from the previous equation depended on the pressure. These were plotted as a function of the relative pressure to obtain the permeability curve of the various HNBR nanocomposite samples (Fig. 6). We clearly observed a noticeable decrease in the permeability of nitrogen gas after the addition of CNTs into the HNBR matrix. Q is the indication of the volume of gas permeated in 1 s for a partial pressure difference of 1 Pa. To obtain a clear picture of the permeability measure-

ments, the permeation coefficients were measured. The values of Q could be taken as the slope of the curves plotted from Figure 6. The slope was measured with linear approximation fitted in the curve. From Figure 6 for various HNBR/CNT samples, the Q values were found to be 59 (HCNT3.5), 62 (HMB3.5), 55 (HMBDA3.5), and 58 (HMBNaDBBS3.5) $\text{cm}^3 \text{ mm m}^{-1} \text{ day}^{-1} \text{ bar}^{-1}$ in comparison to the control sample, which had a Q of 88 $\text{cm}^3 \text{ mm m}^{-1} \text{ day}^{-1} \text{ bar}^{-1}$. There was a remarkable reduction in the permeation levels up to 37.5%. This investigation suggests that thin nanotubes formed a tortuous path for the diffusion of gas in the rubber matrix, which resulted in a significant reduction in the permeability.

With the use of DA and NaDBBS, there was a further reduction in Q ; this indicated a more uniform and enhanced dispersion of nanotubes in the HNBR matrix. One of the major factors for reducing the permeability of gases is the formation of strong matrix–filler networks. From our earlier DMTA investigations, we observed improved crosslinks between the filler and the matrix. With the increase in filler network, the rubber became trapped with fillers; this, thereby, effectively increased the filler volume fraction. This lowered the mobility of the polymer chains, which resulted in a considerable decrease in the diffusion of nitrogen. Also, the possible explanation for the further reduction in gas permeability with the use of various coupling agents could have been the increased interchain attraction due to the predispersion of CNTs. This might have resulted in a highly impermeable surface due to closer spacing between the filler and the rubber chain molecules.

It is also worth pointing out that the roles of the polymer chain constitution,¹⁷ the nature, shape, and size of the permeate,^{18,19} and the influence of the fillers^{12,18,19} need to be considered for the permeability of gases. It is well known that the presence of polar groups in polymer molecules generally reduces the permeability of the polymers, whereas there will be

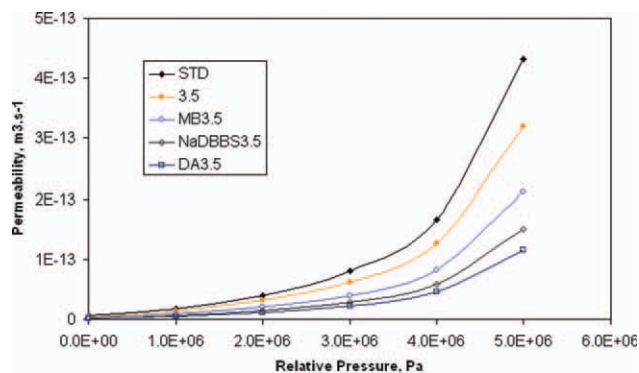


Figure 6 Nitrogen permeability of the various HNBR/CNT nanocomposites (STD, Control Sample MB, masterbatch). [Color figure can be viewed in the online issue, which is available at wileyonlinelibrary.com.]

an opposite effect with the presence of double bonds.²⁰ HNBR, having an ACN content, is polar in nature and has intermolecular and intramolecular CN dipole interactions in the rubber matrix.²¹ This interaction increased the density of the polymer chain matrix and, thereby, decreased the free volume in the rubber matrix.²¹ This, consequently, decreased the solubility of hydrocarbons in HNBR and, thereby, reduced the sorption of gases.

CONCLUSIONS

HNBR nanocomposites filled with CNTs were prepared by two different processing methods at different percentages of nanotubes. The structural, mechanical, and viscoelastic properties and gas permeability behavior of the processed nanocomposites were studied. A loading level of 3.5 phr CNT in both methods of direct addition and masterbatch technique gave rise to an optimal dispersion of the filler into the elastomer matrix, as verified from various described analyses. The surfaces of the CNTs were modified with suitable surfactant and DA. Improved compatibility was observed with the aid of surface modifiers and the predispersion of CNTs in HNBR. TEM analysis revealed better and more uniform dispersion of CNTs in the HNBR matrix after the use of various coupling agents. For 3.5 phr levels of CNTs prepared by the direct addition of CNTs to the mixer, the tensile strength increased by 7.5%, and the modulus increased by 65.5%. The elongation at break was not much affected. After use of suitable coupling agents, the tensile strength, modulus, and elongation at break increased by 5, 60, and 7.7%, respectively. This clearly showed improved adhesion of CNTs onto the rubber chains by the use of predispersion techniques. The viscoelastic behavior revealed an increased E' and increased T_g . Permeability studies showed a reduction in the permeability of nitrogen gas by 37.5%. The investigations revealed that to enhance the compatibility of the CNTs and elastomer, the master-

batch technique was the desirable and preferred method to tailor and balance the required properties.

The authors are grateful for the assistance and support of P. Warren, A. Douglas, and S. Winterbottom for use of the facilities and expertise in processing the final samples at James Walker Co., Ltd.

References

1. Alexandre, M.; Dubois, P. *Mater Sci Eng R* 2000, 28, 1.
2. LeBaron, P. C.; Wang, Z. *Appl Clay Sci* 1999, 15, 11.
3. Misra, R. D. K.; Nerikar, P. *Mater Sci Eng A* 2004, 384, 284.
4. Iijima, S. *Nature* 1991, 354, 56.
5. Ando, Y.; Zhao, X.; Shimoyama, H.; Sakai, G.; Kaneto, K. *Int J Inorg Mater* 1999, 1, 77.
6. Hernande, E.; Goze, C.; Bernier, P. *Phys Rev Lett* 1998, 80, 4502.
7. Berber, S.; Kwon, Y. K.; Tonmanek, D. *Phys Rev Lett* 2000, 84, 4613.
8. Akbar, S.; Beyou, E.; Cassagnau, P.; Chaumont, P.; Farzi, G. *Polymer* 2009, 50, 2535.
9. Verge, P.; Peeterbroeck, S.; Bonnaud, L.; Dubois, P. *Compos Sci Technol* 2010, 70, 1453.
10. López-Manchado, M. A.; Biagiotti, J.; Valentini, L.; Kenny, J. M. *J Appl Polym Sci* 2004, 92, 3394.
11. George, S.; Ninan, K. N.; Groeninck, G.; Thomas, S. *J Appl Polym Sci* 2000, 78, 1280.
12. Wang, M. J. *Rubber Chem Technol* 1998, 71, 520.
13. Sui, G.; Zhong, W. H.; Yang, X. P.; Yu, Y. H. *Mater Sci Eng A* 2008, 485, 524.
14. Vu, Y. T.; Mark, J. E.; Pham, L. H.; Engelhardt, M. *J Appl Polym Sci* 2001, 82, 1391.
15. Vaisman, L.; Wachtel, E.; Wagner, H. D.; Marom, G. *Polymer* 2007, 48, 6843.
16. Felhös, D.; Karger-Kocsis, J.; Xu, D. *J Appl Polym Sci* 2008, 108, 2840.
17. Brydson, J. A. *Rubbery Materials and Their Compounds*; Elsevier Applied Science, London, UK, 1988.
18. Kreiselmair, R. *Kautsch Gummi Kunst* 2002, 06, 316.
19. Georgoulis, L. B.; Morgan, M. S.; Andrianopoulos, N.; Seferis, J. C. *J Appl Polym Sci* 2005, 97, 775.
20. Plastic Design Library Staff: *Permeability and Other Film Properties of Plastics and Elastomers*; William Andrew Publishing/Plastics Design Library Norwich, NY, USA, 1995, p 467.
21. Yang, X.; Giese, U.; Schuster, R. H. *Kautsch Gummi Kunst* 2008, 06, 294.